

Available online at www.sciencedirect.com

ScienceDirect

www.elsevier.com/locate/jes

JES
JOURNAL OF
ENVIRONMENTAL
SCIENCES
www.jesc.ac.cn

Palm oil biodiesel: An assessment of PAH emissions, oxidative potential and ecotoxicity of particulate matter

Silvana Arias¹, Francisco Molina¹, John R. Agudelo^{2,*}

¹Grupo de Investigación en Gestión y Modelación Ambiental -GAIA, Escuela Ambiental, Facultad de Ingeniería, Universidad de Antioquia UdeA, Calle 70 No.52-21, Medellín, Colombia

²Departamento de Ingeniería Mecánica, Universidad de Antioquia UdeA

ARTICLE INFO

Article history:

Received 20 May 2020

Revised 19 August 2020

Accepted 20 August 2020

Available online 11 September 2020

Keywords:

Biodiesel

Particulate matter

P emissions

Oxidative stress

Ecotoxicity

Daphnia pulex

ABSTRACT

This work assessed the impact of fuelling an automotive engine with palm biodiesel (pure, and two blends of 10% and 20% with diesel, B100, B10 and B20, respectively) operating under representative urban driving conditions on 17 priority polycyclic aromatic hydrocarbon (PAH) compounds, oxidative potential of ascorbic acid (OP^{AA}), and ecotoxicity through *Daphnia pulex* mortality test. PM diluted with filtered fresh air (WD) gathered in a minitunnel, and particulate matter (PM) collected directly from the exhaust gas stream (W/oD) were used for comparison. Results showed that PM collecting method significantly impact PAH concentration. Although all PAH appeared in both, WD and W/oD, higher concentrations were obtained in the last case. Increasing biodiesel concentration in the fuel blend decreased all PAH compounds, and those with 3 and 5 aromatic rings were the most abundant. Palm biodiesel affected both OP^{AA} and ecotoxicity. While B10 and B20 exhibited the same rate of ascorbic acid (AA) depletion, B100 showed significant faster oxidation rate during the first four minutes and oxidized 10% more AA at the end of the test. B100 and B20 were significantly more ecotoxic than B10. The lethal concentration LC50 for B10 was 6.13 mg/L. It was concluded that palm biodiesel decreased PAH compounds, but increased the oxidative potential and ecotoxicity.

© 2020 The Research Center for Eco-Environmental Sciences, Chinese Academy of Sciences. Published by Elsevier B.V.

Introduction

From the diesel emissions scandal, in which some vehicle manufacturers intentionally manipulated the electronic control unit of their engines to comply with the current strict legislation, the reputation of diesel vehicles has come under strong criticism. Furthermore, it has been reported that their

emissions cause cancer, as confirmed by international agencies devoted to the assessment of the impact of carcinogens on human health (IARC et al., 2012). These major concerns have undermined the general acceptance of diesel engines and allowed this matter to be heavily politically charged. In response to this situation, new proposals, which are still under discussion, have emerged in the short term to replace diesel-powered vehicles with electric or hybrid engines. At the

* Corresponding author.

E-mail: john.agudelo1@udea.edu.co (J.R. Agudelo).

Table 1 – Engine specifications and engine operating modes.

Type and Configuration		Cummins ISF 2.8, 4 stroke, common rail, split and direct injection, 4 cylinders in line, turbocharged, intercooler, diesel oxidation catalyst (DOC) and cooled EGR		
Compression ratio		17.5:1		
Displacement (L)		2.8		
Bore/Stroke (mm)		94/100		
Maximum Power (kW at r/min)		120 at 3600		
Maximum Torque (Nm at r/min)		360 at 1800		
Engine operating modes representative of urban driving conditions				
Mode	Rotational speed (r/min)	Torque (Nm)	Vehicle speed (km/hr)	VSP (W/kg)
MM	2200	90	59.4	8.8
HM	2800	80	26.3	2.8

same time the interest in new non-conventional “clean” fuels, such as hydrogen, as a fossil substitute has gained interest (Reitz et al., 2020).

Biodiesel has been introduced as an alternative fuel blended with petrochemical diesel to reduce diesel PM emissions due to its oxygen content and because it lacks of aromatics and sulfur in its composition (Fontaras et al., 2010; Guan et al., 2017; Lapuerta et al., 2008). There still exist concern on the organic compounds of PM coming from biodiesel, because although they do not contribute significantly to the mass of the particulates, they might increase significantly its toxicity since biodiesel PM contains more water-soluble non-polar and polar organic compounds than diesel (Gali et al., 2017) suggesting the necessity of assessing the toxicity of that PM.

There is no consensus regarding the PAH emissions and toxicity of biodiesel PM (Bakeas et al., 2011; Borillo et al., 2018; Karavalakis et al., 2010, 2011; Vojtisek-lom et al., 2012; Zhang et al., 2019). These contradictions may be due to several factors such as differences in biodiesel composition, type of engine technology and operating modes, driving cycle, as well as the method of collecting the PM, which consist on the dilution (WD) or not (W/o/D) of the exhaust gases stream with pure air. With regard to the effect of PM collecting methodology, Martin and co-workers (Martin et al., 2017) reported differences in PAH concentration and nitro PAH composition when PM was collected directly from the tailpipe exhaust system (W/oD) with respect to that collected from the breathing zone after undergoing natural dilution processes.

The health affection caused by PM is attributed to oxidative stress at the cellular level, which induces activation of antioxidant defense and inflammations. The oxidative potential (OP) of PM induce the production of reactive oxygen species (ROS), and has been investigated using cellular (in vivo and in vitro) and acellular methods like the antioxidant depletion (Ayres et al., 2008; Calas et al., 2018). The ascorbic acid (AA) depletion test OP^{AA} , is commonly used to assess OP, since AA it is the most abundant antioxidant found in lung fluids (Pietrogrande et al., 2019).

On the other hand, once generated in the combustion process, the PM may transport environmental substances to air, water, soil and aquatic sediments. Given this, it is also necessary to evaluate the water-soluble fraction (WSF) of the PM (Liu et al., 2020; Zou et al., 2016). Aquatic invertebrates such as the *Daphnia pulex* (*D. pulex*) have been used as a way to assess the oxidative stress of the WSF from different compounds and

pollutants (Nikinmaa et al., 2019; Volta et al., 2020). This microcrustacean specie is an integral part of freshwater ecosystems. They are often used in ecotoxicology studies because of their sensitivity to environmental changes, wide geographical distribution and genetic homogeneity (Colbourne et al., 2011; Liu et al., 2018).

The discussion above inspired us to assess several key parameters such as the PM collecting method, the oxidative potential through AA, and the eco-toxicity with *D. pulex* of the PM coming from palm oil biodiesel in an automotive diesel engine, which in the authors knowledge are still unknown. Inspired on this, we focus on assessing the impact of diluting and non-diluting exhaust stream gases, and increasing biodiesel blend ratio from 10%, 20% with diesel fuel and pure 100% biodiesel, on the emissions of 17 PAH compounds. Additionally, non-diluted PM was used to assess its oxidative potential through ascorbic acid assay, and its eco-toxicity through *D. pulex* mortality.

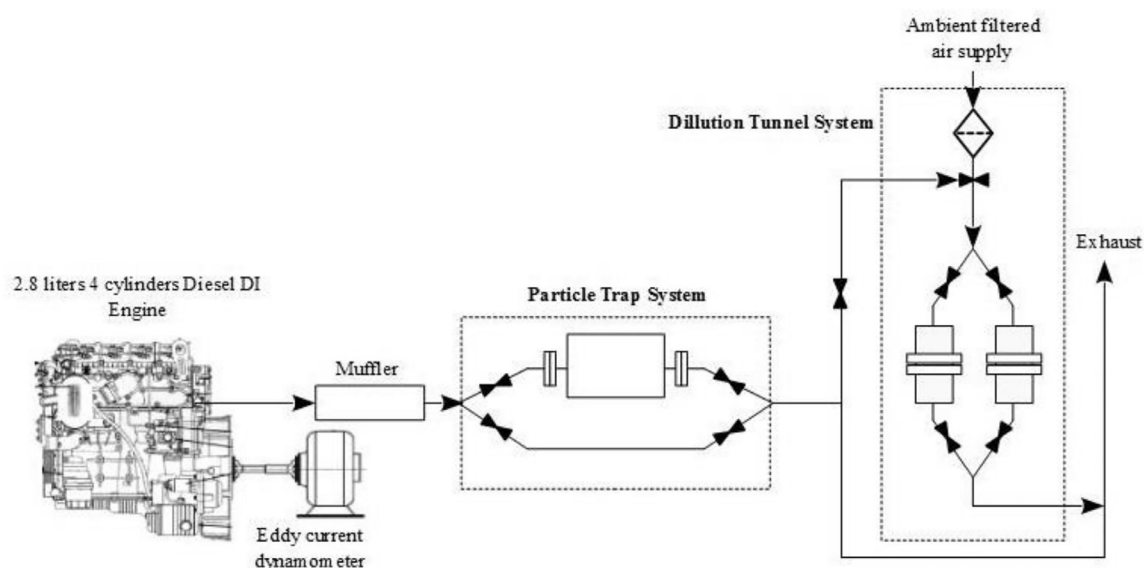
1. Materials and methods

1.1. Diesel engine and testing fuels

The experiments were carried out in an automotive, common rail, turbocharged and intercooled Cummins ISF 2.8 L diesel engine (Euro 4 emissions standard). This high pressure, split injection, non-diesel particulate filter engine was equipped with an oxidation catalyst (DOC) and with a cooled EGR system. The torque output of the engine was regulated by adjusting an eddy current dynamometer brake (E90, Schenck, Germany) and tested in two steady-state operating modes. The main characteristics of the engine are listed in Table 1. Engine operating modes correspond to medium load (MM: 2200 r/min and 90 Nm) and high load (HM: 2800 r/min and 80 Nm), and they were selected as the most representative of urban driving conditions in a frequency approach by means of longitudinal dynamics analysis and the Vehicular Specific Power (VSP) methodology of the pickup truck simulated with the World-wide harmonized Light duty Test Cycle (WLTC). Although with a small engine speed variation range of only 600 r/min, both MM and HM engine operating modes were stable and repeatable during operation in the test rig, and moreover, they are highly representative of urban driving conditions with markedly different vehicle speed and vehicle spe-

Table 2 – Fuel properties.

Property	Method	ULSD	B10	B20	B100
Density at 15 °C (kg/m ³)	ASTM D4052–15	851	854.0	856.0	875.4
Kinematic viscosity at 40 °C (mm ² /sec)	ASTM-D445–17a	3.125	3.462	3.731	4.467
Lower heating value (MJ/kg)	ASTM D240–09	42.43	41.9	41.5	37.9
Water content (mg/kg)	ASTM E203–16	102	123	138	155
Cloud point (°C)	ASTM-D2500:2017a	–5	–3	6	12
Initial boiling point (°C)		168	168.5	187.5	302
95% (V/V) recovery (°C)	ASTM D86:2018	360	358.5	348.7	–
Final boiling point (°C)		389	370.5	359.3	348.0
FAME content (% mass)	UNE-EN 14,078:2014	–	9.85	20.2	97.2
Monoaromatics (% mass)	DIN	–	21.9	18.4	–
Diaromatics (% mass)	EN	–	–	1.9	–
Triaromatics (% mass)	12,916:2016	–	–	0.1	–
PAH content (% mass)		–	3.1	2.0	–
Total aromatics (% mass)		31.5	25.0	20.4	–
Cetane number	DIN EN 17,155:2018	45	47.9	49.4	69

**Fig. 1 – Engine setup for PM collection.**

cific power –VSP– (Table 1). The VSP (kW/ton), defined as the instantaneous power required to overcome the kinetic and potential energy and aerodynamic drag, per unit of vehicle mass, depends highly on vehicle speed, acceleration and road grade, and has shown to be a key parameter in order to compare pollutant emissions (Liu and Barth, 2012).

The engine was instrumented with temperature and pressure sensors (before and after of the compressor and turbine, lube oil, fuel, etc.). For the thermodynamic combustion diagnosis, in-cylinder pressure was measured with a piezoelectric pressure transducer (6056A, Kistler, Germany) coupled to a charge amplifier (5011B, Kistler, Germany). Crankshaft rotational speed and instantaneous piston position were determined with an angle encoder providing 1024 pulses/rev (ROD 426, Heidenhain, Germany). A total of 100 pressure curves, and 3 repetitions were registered at each operating mode to guarantee reliability in combustion diagnosis results. Air consumption was acquired directly from engine's electronic con-

trol unit and fuel consumption was determined with an electronic weight scale (AUW120D ± 0.01 mg, Shimadzu, Japan).

Three fuels were evaluated in this experimental study. Pure palm oil biodiesel (B100), and two blends of 10% (V/V) biodiesel (B10) and 20% (V/V) biodiesel (B20) with ultra-low diesel fuel (Table 2). These biodiesel blends were chosen as highly representative since they have shown to provide good balance between cold weather operability, performance and emission benefits. In addition, elsewhere it has been reported that both B10 and B20 blends can be used in most diesel engines without modifications (U.S. Department of Energy, 2004).

1.2. Particulate matter collecting methods

1.2.1. Without dilution (W/oD)

PM samples were collected in a particle trap (Fig. 1) filled with stainless-steel wools installed in the exhaust pipe, right after the muffler at 1.5 m downstream the exhaust turbine, keep-

ing the temperature below 200°C to avoid oxidative reactions on PM. Two pressure sensors before and after the trap were installed to guarantee a maximum pressure drop of around 8 kPa during PM collection, close to that recommended for diesel particulate filters avoiding any backpressure affecting engine operation (Lapuerta et al., 2012b).

1.2.2. With dilution (WD)

PM samples were collected cooled in a partial dilution (Fig. 1) mini tunnel (Ricardo™, UK) and diluted onto conditioned 47 mm diameter micro fiberglass filters (GC 50, ADVANTEC, USA, porosity 0.50 μm) installed at the exit of the exhaust pipe. The dilution ratio (4:1) was calibrated by means of NO_x concentration (in ppm) measured before and after the dilution system. A temperature of around 52°C was guarantee during PM collection process. This dilution ratio is commonly limited as the lowest allowed for PM measuring protocol recommended by international standards, it was selected in this work because of the high mass of particulates with the minimum fuel consumption gathered from the test.

1.3. PAH extraction and analysis

Depending on PM availability and plausibility tests, among 6 to 9 samples were extracted and analyzed from each tested fuel. All extractions were carried out with 1 filter in a 66 mL stainless steel vessel using an ASE 300 system (Dionex® Thermo Scientific, PA, USA). The stagnant volume of each vessel was filled with diatomite and the extraction was performed with water and methanol (3:1), the latter as a disperser solvent, the temperature was 200°C and 5 min of static times at a high-pressure of 10,000 kPa (Ramos-Contreras et al., 2019). The obtained solution was collected and used in the Dispersive liquid–liquid microextraction procedure (DLLME).

For the DLLME, 1000 μL of hexane was injected rapidly into a vial containing 50 mL of sample solution from ASE extraction. Then, the vial was sealed; the cloudy solution formed was vortexed for 180 s to distribute extractor solvent through the solution. Then, centrifugation at 3500 r/min for 240 sec was applied to separate organic phase from aqueous solution. The top phase was taken and injected into the GC/MS system.

Analysis was performed on a gas chromatograph (TRACE GC Ultra, Thermo Scientific, USA) coupled to a mass spectrometer (ISQ, Thermo Scientific, USA). Ultra-pure helium (99.9999%) was used as carrier gas at a constant flow rate of 1.5 mL/min, the volume injected was 1 μL in splitless mode with a pressure pulse. Injection temperature was 280°C, the ion source was electron impact (EI) mode, source temperature 275°C, and mass selective detector (MSD) transfer line 300°C.

Chromatographic separation was performed on an Agilent J&W Select PAH column (CP 7462), 30 m \times 0.25 mm \times 0.15 μm . The oven temperature was programmed as follows: 70°C for 0.8 min, ramping 60°C/min to 180°C, 5°C/min to 300°C and finally ramping 1°C/min to 320°C for 2 min. Total run time was 48.63 min.

1.4. Oxidative potential of ascorbic acid depletion test (OP^{AA})

The OP^{AA} assay was used in this work because it has shown better correlation with the production of intracellular reactive oxygen species than other oxidative tests, and because it has been reported as reliable to predict biological effects driven by PM based on oxidative stress (Crobeddu et al., 2017). The PM solutions were prepared by weighing 3 mg of PM. Due to the limited amount of PM available, this test was performed only for the samples collected in MM (2200 r/min and 90 Nm). Each PM sample was added to a falcon tube with 2 mL of methanol, vortexed for 10 min, and exposed to ultrasonic waves for one minute. PM suspensions were concentrated to less than 1 mL in constant nitrogen flow at 30°C and suspended with water with conductivity less than 0.05 $\mu\text{S}/\text{cm}$ at a concentration of 600 $\mu\text{g}/\text{mL}$.

Samples were diluted to an initial concentration of 12.5 $\mu\text{g}/\text{mL}$ before incubation with AA. Tests were performed by triplicate. The exposures were initiated by adding 1.3 mL of an AA solution (2 mM) in a 50 mm rectangular glass cell containing 1.3 mL of water and 10.4 mL of PM suspension, at initial AA concentrations of 200 μM and 10 $\mu\text{g}/\text{mL}$ of PM. The test cell was pre-incubated for 10 min at 37°C immediately before the addition of AA.

After AA addition, the remaining concentration in each cell was monitored every two minutes for a period of two hours by measuring the absorbance at 265 nm in a UV–VIS spectrophotometer (Pharo 300 Spectroquant®, Merck, USA). In order to control the contribution of the absorbance of the PM themselves, free of AA, two controls containing 2.6 mL of water with conductivity less than 0.05 $\mu\text{S}/\text{m}$ and 10.4 mL of the individual particle suspension were performed and subtracted from the absorbance of the samples. Acid ascorbic concentrations were determined by a calibration curve. From these data, the rate of AA depletion associated with the sample minus that observed in the appropriate blank was derived. Results are presented as AA depletion percentage versus time.

1.5. Acute ecotoxicity tests with *Daphnia pulex*

Ecotoxicity tests have shown to be a potential tool to evaluate the toxicology risk on living organisms, before carrying out specific in vitro or in vivo tests with human cells (Roig et al., 2013). *D. pulex* is an important aquatic invertebrate for risk assessment and is considered a sentinel organism for environmental problems (Chain et al., 2019) because their genes are sensitive to environmental changes (Colbourne et al., 2011). Although most studies assessing the biological activity of PM have used the soluble organic fraction (SOF), in this work, the WSF was preferred since it turns out to be highly toxic for these aquatic organisms.

In this study, four replications and a total of 20 infants of *D. pulex* were used in each treatment or exposure level. The tests were carried out under a static system without renewal of the solutions for 48 hr. The strain of *D. pulex* was collected in La Fe freshwater reservoir (Medellín rural area-Colombia). The cultures were maintained in the laboratory at $20 \pm 2^\circ\text{C}$ with a photoperiod of 16 light hours and eight hours of darkness and lighting with 538 to 1076 lx. The concentration of dissolved

oxygen was maintained at a level greater than 60% saturation. *D. pulex* infants were fed up to two hours before the test. For three days a 1.5 mL/L of food was supplied to the cultures. For this experimental study, 24-hour-old *D. pulex* infants extracted from the mass cultures were used.

As for the oxidative potential of ascorbic acid depletion test, the assessment of acute ecotoxicity of PM was performed only to the samples collected in MM. The extractable material from the particulates for ecotoxicity test was obtained by preparing a solution of PM in reconstituted water at a concentration of 10 mg/L, ultrasound extraction was performed for three hours, and filtered seven times on fiberglass filters (GC 50, ADVANTEC, USA, porosity 0.50 μm) until not difference between leaks was observed. A total of 360 infants (120 per test) were captured. Different solutions in reconstituted water were prepared as: Treatment 1, 2, 3, 4 by dilutions from the filtered sample with sample fraction (in% by volume) of 12.5, 25, 50, 100. A total volume of 100 mL was used for all treatments. A positive and negative control were performed. The first, allowed to evaluate the sensitivity of the strain, while the last one stated the reference for comparison. The same dilution water for preparing the samples was employed as negative control, while the positive control was performed with a solution of potassium dichromate in a concentration corresponding to the average of the lethal concentration at 50% mortality (LC_{50}) calculated according to the last sensitivity control chart of the strain.

The results of the acute ecotoxicity tests constitute an approximation to the lethal effect of short exposures of living organisms to toxic substances or to environmental factors. With different levels of exposure (dilutions of the sample -PM water extract-) the mean lethal concentration (LC_{50}) was determined as the end point for the test time, that is, the concentration or dilution of the sample inducing a lethal effect on 50% of the exposed specimens. LC_{50} was calculated with a Probit analysis (Finney, 1971). The smaller the amount required to reach LC_{50} , the greater the toxicity of the sample.

2. Results and discussion

2.1. Combustion diagnosis

Fig. 2 shows the thermodynamic combustion diagnosis for both engine operating modes (MM: left and HM: right). The combustion history remains very close for all fuels tested, with a small amount of heat released from the pre-injection, and a main heat release from main injection. Despite the piezoelectric injector used by this engine, a clear advance in heat release timing is evident for B100 in both operating modes, which is usually due to higher cetane number (Benjumea et al., 2011) and to a less extent also due to higher compressibility bulk modulus of biodiesel compared to diesel fuel (Lapuerta et al., 2012a). Fig. 2 evidenced that maximum instantaneous in-cylinder average bulk temperature is about 100 °C higher in HM than in MM, and additionally that although at MM they were very similar, at HM both B20 and B100 blends exhibited higher maximum temperature, as well, as higher heat release rate than B10 fuel, this may be due to the unmodified conditions of the electronic control unit, which

was optimized by the manufacturer for B10. As the concentration of biodiesel is increased the lower heating value of the fuel blend is decreased, and more fuel shall be injected to keep the engine power output constant in a specific engine operating mode (Benjumea et al., 2009), due to this, more amount of biodiesel is burned during the diffusion combustion phase (Fig. 2 bottom), which may induce high maximum in-cylinder temperature.

The heat release fraction (Cumulative heat release) in Fig. 2 shows similar average bulk in-cylinder combustion performance for all fuels independently of the engine operating mode, in addition, this shows that the combustion reach above 99% of the total heat released after 60 crank angle degrees, which is common in diesel engine combustion. The rest of this unburned fuel could be one of the components conforming the particulate matter, which may help to explain the content of PAHs measured in the PM (Williams, Bartle, and Andrews, 1986).

2.2. PAH emissions by number of aromatic rings

Fig. 3 shows the mass-based distribution of PAH by number of aromatic rings for all tests. Independently of PM collecting method (WD or W/oD), engine operating mode (HM and MM), and fuel type, the 5 aromatic ring compounds prevailed over others, followed by 3 and then 4 rings. Similar results for PM coming from diesel combustion in general have been reported in literature for diesel PM (Bakeas et al., 2011; Borillo et al., 2018; Corrêa and Arbilla, 2006). It is likely that light PAHs (3 rings and less) could be mainly contained in the gas phase not analyzed in this work, while the HMW PAHs which have higher boiling points (4 rings and more) can be physically adsorbed on the particle surfaces (Alvarez et al., 2017; Ballesteros et al., 2010; Callén et al., 2008). In a recent work, authors collected both gas and particle phases under real-driving conditions on-board of a EURO IV diesel truck, fuelled with B10, B20 and B100, and found that the most abundant PAH in the particle-phase are 3 ring and 5 ring structures. However, in the gas phase a large increase in 2-ring PAH emission is observed while those with 3 and 4 rings decrease for most cases (Botero et al., 2020).

Pyrolysis and pyrosynthesis of heaviest n-alkanes are two main mechanisms that can explain the formation of PAH in rich fuel regions evolving the diesel flame (Ravindra et al., 2008). Traces of unburned fuel and lubricating oil have also been suggested as sources of PAH in diesel combustion (Li et al., 2008). PAH of 5 and 6 aromatic rings could be formed by the addition of hydrocarbon radicals to LMW PAH through the mechanism of formation of alkyl PAH (Wiersum, 1996). However, in the case of biodiesel (aromatics-free fuel), PAH are mainly formed by thermal polymerization processes of the fatty acid methyl esters that form cyclohexane, therefore, hydrogen abstractions reactions from the cyclohexene rings and stable aromatics could subsequently form (Ratcliff et al., 2010). In addition, the temperature transition from the exhaust system (high) to the minitunnel (low) could undergo PAH transformation/condensation on PM surface, for example, PAH nitration reactions (Arey et al., 1986; Carrara et al., 2010).

For B10 and B20, the most abundant PAH are those with 3 and 5 ring structures, although 3-ring compounds should be distributed mostly in the gas phase (Masih et al., 2012). One

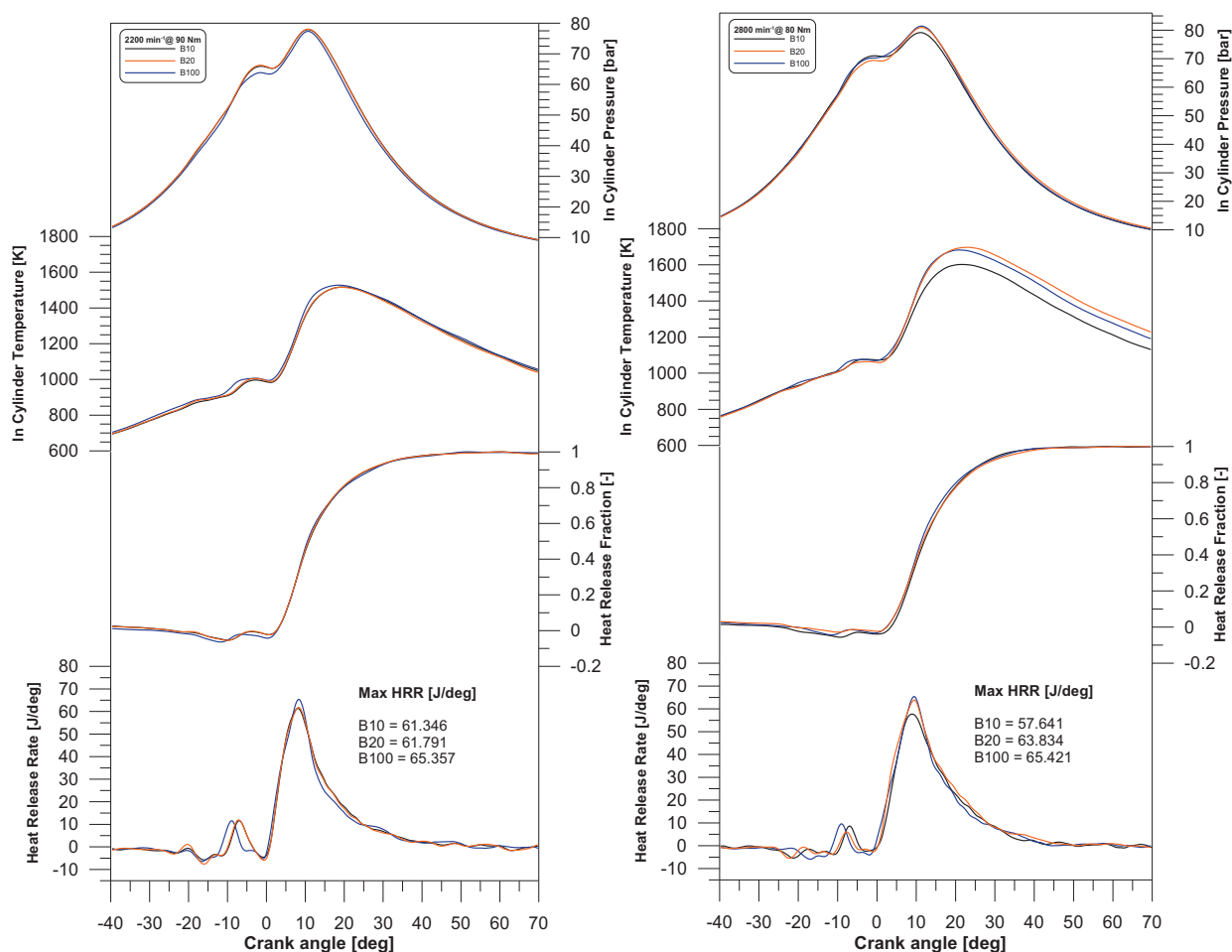


Fig. 2 – In-cylinder combustion parameters. Left: MM, right: HM.

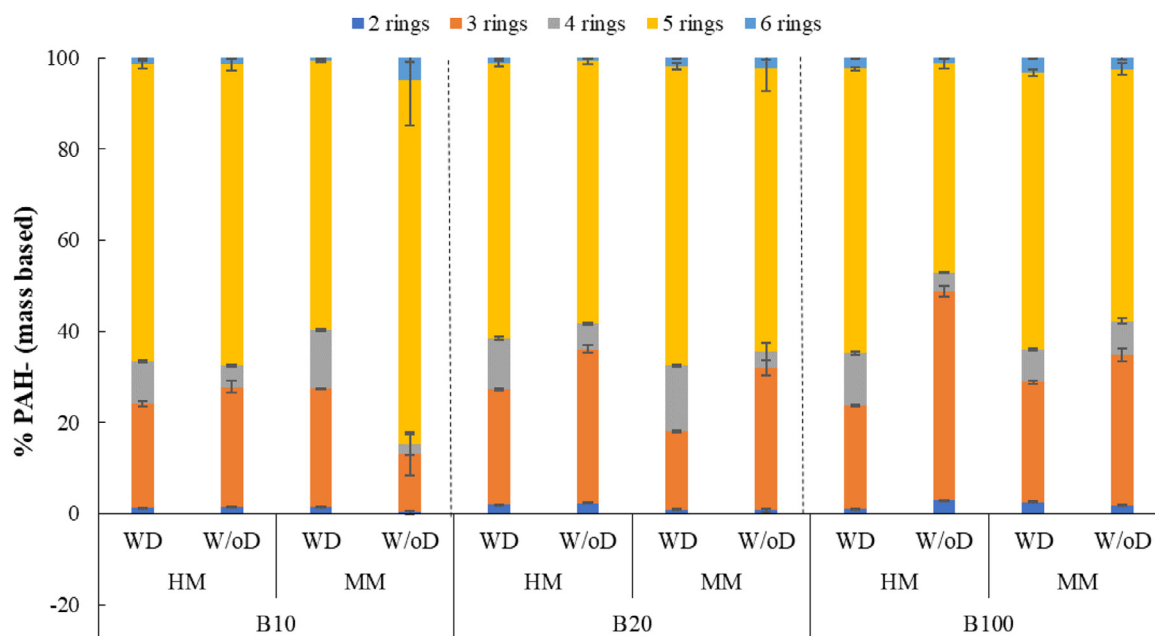


Fig. 3 – Mass-based distribution of 17 PAHs by number of aromatic rings for the three fuels and two operation modes tested, W/oD and WD.

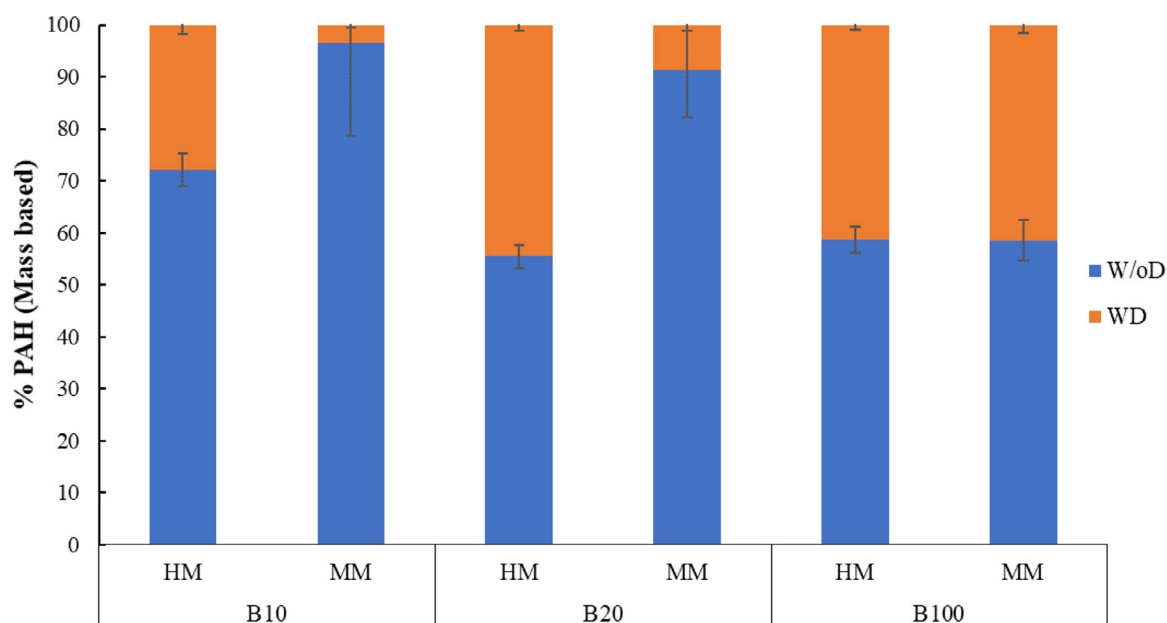


Fig. 4 – Percentage distribution of emitted 17 PAHs according to collection methods.

of the most abundant 3-ring compounds was phenanthrene which has also been reported as abundant in PM from diesel and diesel-biodiesel blends emissions (de Souza and Corrêa, 2016; Karavalakis et al., 2010; Li et al., 2018). As mentioned previously, the formation of the 5 rings PAHs could be due to the pyrosynthesis of low molecular weight aromatic compounds which seems to be dominant over the LMW PAH formation that can be pyrolyzed by incomplete combustion of the fuel. The order from the highest to the lowest concentration of the 5 aromatic ring PAH measured was: Benzo[b]fluoranthene > benzo[k]fluoranthene > benzo[a]pyrene > benzo[e]pyrene. These HMW PAH have also been reported as the most abundant ones in environmental air samples by other researchers (Mueller et al., 2019; Paulo et al., 2019) in the Medellín metropolitan area, where the use of palm oil biodiesel B10 blend is mandatory, and several last mile cargo fleets voluntary use a B20 blend. Rojas et al. reported high concentration of 5 and 6 aromatic rings PAH in an old out of service engine operating with B15 (15% of palm oil biodiesel blended with diesel fuel) at idle conditions (Rojas et al., 2011). Fig. S1 in supplementary material shows the specific emissions of the 17 PAH ($\mu\text{g}/\text{kWh}$) measured in this work.

2.3. Impact of PM collection method and engine operating mode

Fig. 4 shows the percentage of PAH distribution emitted according to collection methods in each engine operating mode and for the three tested fuels. Independently of engine load and fuel tested, much higher levels of PAH emissions were observed when PM was collected without dilution (W/oD) compared to the dilution (WD) collection method. Our results are in agreement with those reported by Lipsky and Robinson (2006) who conducted experiments to examine the effects

of exhaust gases dilution on mass emissions of fine particles and semi-volatile compounds from a diesel engine. They found that at low dilution semi-volatile species are found in large proportion in the particle phase, but the increase in dilution reduced the concentration of semi-volatile species, changing this material to the gas phase to maintain the phase equilibrium.

The reduction of all 17 PAH compounds when changing the method of collection has been attributed to the heterogeneous reactions of PAHs with air. Among other explanations, it has been reported that the dilution with air increases the availability of nitrogen for the conversion of PAH into its nitrated forms. Nitro-PAH could also be formed by reacting PAH with NO_3^- or NO_2^- already associated with particles (Ringuelet et al., 2010).

Pitts et al. (1978) reported that there is a significant effect on PAH concentrations when samples are collected in filters, after dilution with air (WD), or powder (W/oD) and that the collection method played a significant role in the amount of carcinogens PAH. They emphasized the easy formation of nitro-PAH mutagenic derivatives by exposure of non-carcinogenic and carcinogenic PAH to nitrogen oxides, which is more likely to happen when the particulate material is diluted with air. Since our work was devoted on the impact of both collection method and biodiesel content on PAH emissions, it is recommended that for fuels comparison the collection of PM samples W/oD is more convenient.

The effect of engine operating mode on PM properties has been widely addressed in literature. Lee et al. (2002) found that variations in engine load were more important for the formation of particulate agglomerates than the engine speed, which accounts for the effect of residence characteristic time available for agglomeration. Mathis et al. (2005) confirmed that engine load has a greater effect than engine speed on the

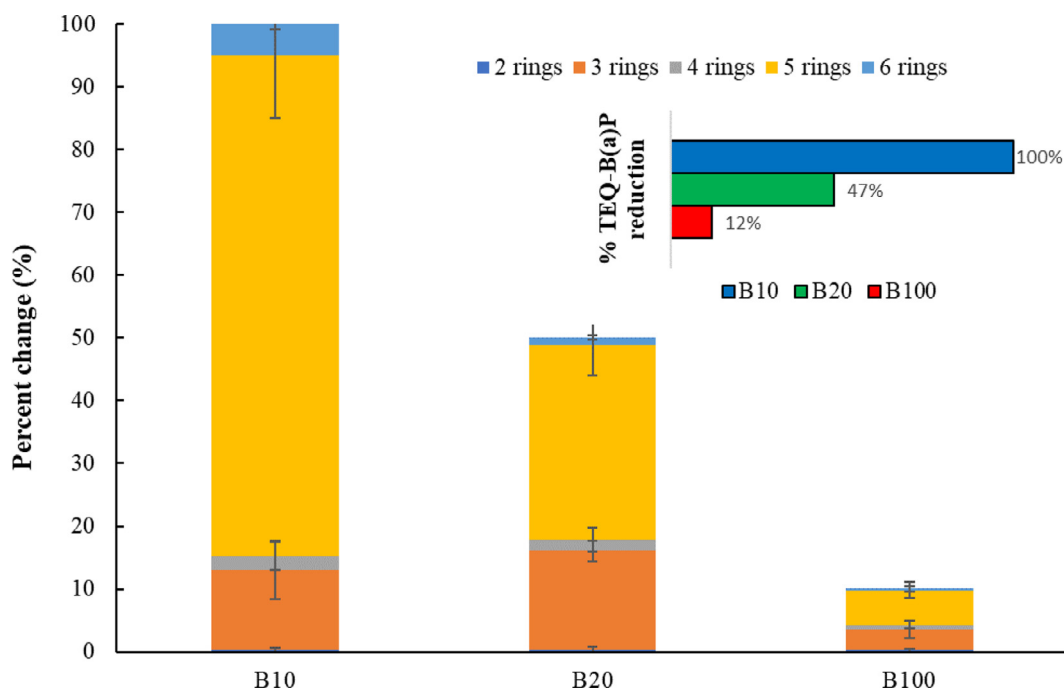


Fig. 5 – Percent of change of PAH by number of rings for the tested fuels at HM (2200 r/min and 90 Nm), W/oD.

size and morphology of the primary soot particles. In previous works authors found that both engine load (Ruiz et al., 2015) and engine speed (Cadrazco et al., 2019) influence the PM composition, morphology and nanostructure, and in consequence its capacity to absorb different type of PAH compounds. In this work engine speed range was 600 r/min, while engine torque varied only 10 Nm between engine operating modes, due to this, it is likely that the residence time would impact at a higher extent than engine torque. The higher PAH emissions obtained in MM with respect to HM (Fig. 4) is in accordance with results reported elsewhere (Bakeas et al., 2011; Ballesteros et al., 2010; Karavalakis et al., 2010; Mi et al., 2000). As engine speed increases, combustion takes place at higher temperatures (Fig. 2) avoiding PAHs to condensate on the particulate surface. Additionally, the pyro synthesis of PAHs could also contribute to burn more PAH compounds, and also high temperatures favors the decomposition of olefins forming PAH precursors (Babushok and Tsang, 2004).

2.4. Impact of palm oil biodiesel concentration on PAH emissions

A total of 17 PAHs were identified and quantified from the PM gathered in the engine exhaust system (see Supplementary Material). Detailed PAH emission reductions were observed W/oD as biodiesel concentration was increased (Fig. 5). B20 exhibited a reduction of around 50% of PAH in comparison with B10, while B100 reduced PAH emissions by 90% compared with B10. These reductions were more pronounced for heavier PAHs (5 and 6 aromatic rings) as shown in Fig. 5. This observation might be due to high molecular weight PAH contributed more to the total PAH emission since they are more likely to

condense during the combustion process (Ballesteros et al., 2010).

The reduction of total PAH obtained with palm oil biodiesel blends is in agreement with the results reported for other biodiesel feedstock (Borillo et al., 2018; Zhang et al., 2019), and might obey to the decrease on aromatic compounds as the biodiesel concentration increases in the fuel blend (see Table 2). The small amount of PAH exhibited by B100 aromatic-free fuel would be related to the formation of aromatics during the complex kinetic reaction pathways taking place in the combustion process, as well as those coming from the lubricating oil (de Souza and Corrêa, 2016).

B(a)P is considered to be one of the most toxic among 17 PAH studied, to calculate the equivalent toxicity (TEQ-B(a)P), the specific toxic equivalent factor (TEF) of individual PAH was used using B(a)P as proposed elsewhere (Nisbet and LaGoy, 1992). As the concentration of biodiesel increased, the TEQ-B(a)P decreased (zoom in Fig. 5). The highest TEQ-B(a)P reduction was found for the B100 (88%) followed by the B20 (53%) with respect to B10. Although from the TEQ-B(a)P results from Fig. 5 it might be inferred that the potential carcinogenicity of PAHs emissions from biodiesel-fueled engine is decreased, this must not be conclusive, since that toxicity index only accounts for the contribution of some specific polycyclic aromatic compounds, but it does not take into account other non-PAH, oxy- and nitro-derivative PAH, among others which are potentially toxic compounds. Furthermore, the calculated TEQ-B(a)P do not account for another type of PAH identified with major toxic effects such as dibenzo(a,l)pyrene, which exhibits a significantly greater carcinogenic potential than the reference benzo(a)pyrene compound (Mahadevan et al., 2005). Li et al. (Li et al., 2018) reported PAH, oxy- and nitro-derivate

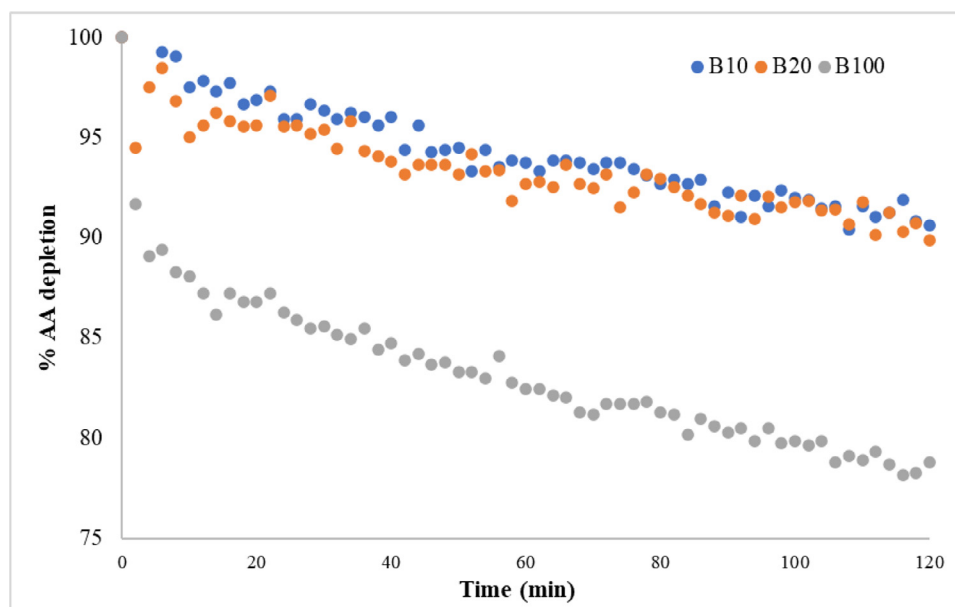


Fig. 6 – Average percentage depletion of AA in 120 min.

PAH emissions from a diesel engine fueled with conventional fossil diesel and waste cooking oil biodiesel using dilution collecting method for the PM. They found that the fractions of parent PAH gradually decrease with increasing biodiesel content in the blends, while the corresponding fractions of oxygenated and nitrated derivatives steadily increase.

Inspired on this, authors investigated the impact of tested PM samples on oxidative potential through the ascorbic acid depletion test, and the assessment of the mortality of *D. pulex*.

2.5. Oxidative potential assessment through ascorbic acid depletion test (OP^{AA})

Every OP^{AA} experiment was replicated 3 times. The average percentage depletion of AA in 120 min for B10, B20 and B100 is shown in Fig. 6. B10 and B20 exhibit the same rate of AA depletion, both reach an oxidation of 10% of the initial concentration of AA.

The slope for the three fuels was similar, however, the B100 fuel exhibited a significant higher oxidation during the first 4 min of the test than the other two fuel blends. From minute 4, the pure biofuel oxidizes at the same rate of B10 and B20. After 120 min of the test, the B100 extract had oxidized 10% more AA than the B10 and B20 extracts. These results are consistent with findings by other authors (Hedayat et al., 2016; Martin et al., 2019; Pourkhesalian et al., 2014) who have investigated the relationship between the oxygen content of different biodiesels and the OP using different reactive oxygen species (ROS) assays and all they concluded that the OP of the PM is strongly related to the oxygen content of the fuel. These OP results may also be related to biofuel properties such as saturation levels of molecules, Pourkhesalian et al. reported that more saturated fuels result in a lower mass of particles but have higher levels of ROS and therefore they would have higher OP (Pourkhesalian et al., 2014).

Godoi et al. evaluated the oxidative stress caused by exposure to PM of diesel and biodiesel (5% and 20%) using the electron spin resonance analysis to measure the free radicals generation. They reported that the higher OH radical emission of soybean oil biodiesel may be responsible for the increase in oxidative potential (Godoi et al., 2016). Additionally, Energy Dispersive X-ray Fluorescence Spectroscopy (EDXRF) employed in their study to determine elemental concentration allowed them to find a strong correlation between metal content, mainly copper and OP.

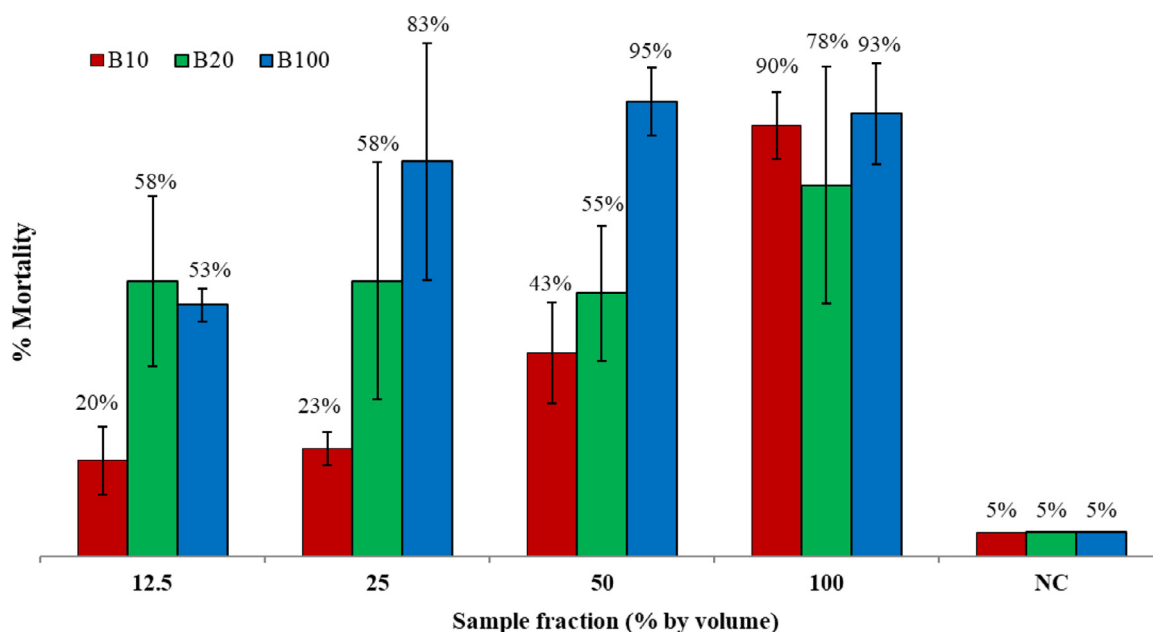
Although PAH can induce oxidative stress indirectly, the composition of the PM from the combustion of biodiesel, diesel or its mixture plays an important role. The oxidative stress cannot be explained by the level of PAH as Hemmingsen et al. claimed in their research (Hemmingsen et al., 2011). There are evidences in literature that different species present in the PM, such as certain polar and non-polar organic compounds and transition metals, among others, can have significant influence on the OP, through the production of ROS (Cheung et al., 2010), resulting in potential damage to cells, inflammations and other adverse health effects (Fang et al., 2019).

2.6. Acute ecotoxicity tests with *Daphnia pulex*

Table 3 shows the results of death or immobility of individuals of *D. pulex* exposed to the sample fractions. B20 and B100 were significantly more toxic than B10, both, induced the mortality of the half of the individuals even with the highest dilution (12.5%). In this case, since the LC_{50} cannot be calculated, then only the non-diluted sample (100% fraction) shall be used for comparison against the negative control (NC). However, the mortality induced by B20 and B100 in all treatments was significantly different from the NC, which means that all sample fractions could be considered adverse effect concentrations,

Table 3 – Immobility or mortality of *D. pulex* neonates exposed for different dilutions of the samples for 48 hrs. PC: positive control, NC: negative control, SD: standard deviation.

Sample	Sample dilution (%)	Dead or immobile per each 20 individuals		SD
		Test 1	Test 2	
B10	12.5	5	3	1.41
	25	5	4	0.71
	50	10	7	2.12
	100	17	19	1.41
	PC	10	8	1.41
	NC	0	1	0.71
B20	12.5	9	14	3.54
	25	8	15	4.95
	50	9	13	2.83
	100	12	19	4.95
	PC	10	8	1.41
	NC	0	1	0.71
B100	12.5	11	10	0.71
	25	13	20	4.95
	50	18	20	1.41
	100	17	20	2.12
	PC	10	8	1.41
	NC	0	1	0.71

**Fig. 7 – Mortality of *D. Pulex* neonates in 48 hrs for PM extracts at MM.**

allowing to conclude that PM extracts from B20 and B100 are highly toxic for *D. Pulex*.

PM from B10 was found to be less toxic to *D. pulex* than B20 and B100. For B10 an increase in the mortality of the individuals was observed as the concentration of the extract increased, therefore, it was possible to determine the LC_{50} -48 hr of 61.32% with a 95% confidence interval from 46.6% to 75.1%, corresponding to a concentration of 6.13 mg/L.

Fig. 7 shows the percentage of mortality for each sample fraction. There was more than 80% of mortality for B100 from 25% to 100% fractions, for B20 the mortality was lower, rang-

ing from 55% to 78% for all sample fractions. From our experimental results it was not possible to obtain the LC_{50} for B20 and B100 PM extracts, from this, it might be inferred that PM coming from palm oil biodiesel in concentrations above 20% (B20) could induce adverse effects on living organisms.

Although for other combustion processes or airborne particulates from urban environments (Jalava et al., 2010; Velali et al., 2018; Vu et al., 2012), our results for PM coming from an automotive diesel engine fuelled with different palm oil biodiesel blends, also demonstrate that there is not necessarily a direct correlation between PAH concentration and

biological activity. Therefore, these adverse effects induced by PM should be associated with other compounds such as PAH reactive derivatives (nitro-PAH, oxy-PAH), quinones (Squadrito et al., 2001) and water-soluble compounds such as trace metals which their biological activity has been studied in atmospheric fine particulate matter (Jiang et al., 2014; Palacio et al., 2016). In addition, other researchers have also suggested that the morphology and nanostructure of the PM would also impact PM oxidative potential (Godoi et al., 2016).

Further investigation to identify these compounds, as well as PM nanostructural characteristics are still an open question in order to identify the impact of the use of palm biodiesel and the associated health risk.

3. Conclusions

Under this test condition and engine configuration consisting of an automotive diesel engine operating at low load (80 Nm – 90 Nm) and at two engine speeds of 2200 and 2800 r/min highly representative of typical urban driving conditions obtained from the WLTC, it can be concluded that as the concentration of palm oil biodiesel was increased, all 17 PAH compounds extracted from the particulate phase decreased significantly, however, both the oxidative potential and the acute ecotoxicity was drastically increased. The following conclusions can be drawn from this experimental research:

1. Higher PAH concentrations were obtained without diluting the exhaust gas stream in comparison with those collected in the minitunnel (WD). To assess the impact of biodiesel concentration on PAH emissions, the collection of non-diluted PM from exhaust gases is preferred over the diluted samples.
2. Independently of the engine operating mode, PAH emissions decreased with palm oil biodiesel concentration. A total of 17 PAH compounds were quantified from the exhaust PM, those with 3 and 5 aromatic rings were the most significant PAH for the three tested fuels (B10, B20 and B100), independently of engine operating modes (MM and HM) and sampling methods (WD and W/oD).
3. The oxidative potential of PM was 10% faster for the PM coming from pure palm oil biodiesel compared to B10, while for B10 and B20 it was similar. These results cannot be explained with the PAH concentration. This motivates to continue researching on the impact of other compounds from biodiesel PM which are contributing to increase the production of reactive oxygen species.
4. The PM coming from palm oil biodiesel proved to be more toxic for *Daphnia Pulex*. This research evidenced that biodiesel promoting policies shall be carefully addressed considering its impact on non-regulated toxic emissions.

Although the two engine operating modes chosen for this experimental work were the most representative of urban driving conditions in the WLTC driving cycle for the vehicle fitted with this specific engine, trends on the PAH emissions, oxidative potential and eco-toxicity of the PM obtained at other engine loads and speeds, or engine types, is still an open question.

Acknowledgments

Authors gratefully acknowledge the financial support provided by the Colombia Scientific Program within the framework of the call *Ecosistema Científico* (Contract No. FP44842–218–2018). Co-author Silvana Arias wish to thank Colombian Ministry of Science and Technology for her PhD scholarship (Bicentenary doctoral excellence scholarship program).

Appendix A. Supplementary data

Supplementary material associated with this article can be found, in the online version, at doi:[10.1016/j.jes.2020.08.022](https://doi.org/10.1016/j.jes.2020.08.022).

REFERENCES

- Alvarez, A., Hernández, J.P., López, A.F., Agudelo, J.R., 2017. Average molecular characterization of the soluble organic fraction of mature diesel particulate matter. *Combust. Flame* 183, 299–308.
- Arey, J., Zielinska, B., Atkinson, R., Winer, A.M., Ramdahl, T., Pitts, J.N., 1986. The formation of nitro-PAH from the gas-phase reactions of fluoranthene and pyrene with the OH radical in the presence of NOx. *Atmos. Environ.* 20, 2339–2345.
- Ayres, J.G., Borm, P., Cassee, F.R., Castranova, V., Donaldson, K., Ghio, A., et al., 2008. Evaluating the toxicity of airborne particulate matter and nanoparticles by measuring oxidative stress potential - A workshop report and consensus statement. *Inhal. Toxicol.* 20, 75–99.
- Babushok, V.I., Tsang, W., 2004. Kinetic modeling of heptane combustion and PAH formation. *J. Propuls. Power* 20, 403–414.
- Bakeas, E., Karavalakis, G., Fontaras, G., Stournas, S., 2011. An experimental study on the impact of biodiesel origin on the regulated and PAH emissions from a Euro 4 light-duty vehicle. *Fuel* 90, 3200–3208.
- Ballesteros, R., Hernández, J.J., Lyons, L.L., 2010. An experimental study of the influence of biofuel origin on particle-associated PAH emissions. *Atmos. Environ.* 44, 930–938.
- Benjumea, P., Agudelo, J., Agudelo, A., 2009. Effect of altitude and palm oil biodiesel fuelling on the performance and combustion characteristics of a HSDI diesel engine. *Fuel* 88, 725–731.
- Benjumea, P., Agudelo, J.R., Agudelo, A.F., 2011. Effect of the degree of unsaturation of biodiesel fuels on engine performance, combustion characteristics, and emissions. *Energy & Fuels* 25, 77–85.
- Borillo, G.C., Tadano, Y.S., Godoi, A.F.L., Pauliquevis, T., Sarmiento, H., Rempel, D., et al., 2018. Polycyclic Aromatic Hydrocarbons (PAHs) and nitrated analogs associated to particulate matter emission from a Euro V-SCR engine fuelled with diesel/biodiesel blends. *Sci. Total Environ.* 644, 675–682.
- Botero, M.L., Mendoza, C., Arias, S., Hincapié, O.D., Agudelo, J.R., Ortiz, I.C., 2020. In vitro evaluation of the cytotoxicity, mutagenicity and DNA damage induced by particle matter and gaseous emissions from a medium-duty diesel vehicle under real driving conditions using palm oil biodiesel blends. *Environ. Pollut.* 265, 1–11, 115034.
- Cadrazco, M., Santamaría, A., Agudelo, J.R., 2019. Chemical and nanostructural characteristics of the particulate matter produced by renewable diesel fuel in an automotive diesel engine. *Combust. Flame* 203, 130–142.
- Calas, A., Uzu, G., Kelly, F.J., Houdier, S., Martins, J.M.F., Thomas, F., et al., 2018. Comparison between five acellular oxidative

- potential measurement assays performed with detailed chemistry on PM₁₀ samples from the city of Chamonix (France). *Atmos. Chem. Phys.* 18, 7863–7875.
- Callén, M.S., de la Cruz, M.T., López, J.M., Murillo, R., Navarro, M.V., Mastral, A.M., 2008. Some inferences on the mechanism of atmospheric gas/particle partitioning of polycyclic aromatic hydrocarbons (PAH) at Zaragoza (Spain). *Chemosphere* 73, 1357–1365.
- Carrara, M., Wolf, J.C., Niessner, R., 2010. Nitro-PAH formation studied by interacting artificially PAH-coated soot aerosol with NO₂ in the temperature range of 295–523 K. *Atmos. Environ.* 44, 3878–3885.
- Chain, F.J.J., Finlayson, S., Crease, T., Cristescu, M., 2019. Variation in transcriptional responses to copper exposure across *Daphnia pulex* lineages. *Aquat. Toxicol.* 210, 85–97.
- Cheung, K.L., Ntziachristos, L., Tzankiozis, T., Schauer, J.J., Samaras, Z., Moore, K.F., et al., 2010. Emissions of particulate trace elements, metals and organic species from gasoline, diesel, and biodiesel passenger vehicles and their relation to oxidative potential. *Aerosol Sci. Technol.* 44, 500–513.
- Colbourne, J.K., Pfreder, M.E., Gilbert, D., Thomas, W.K., Tucker, A., Oakley, T.H., et al., 2011. The ecoresponsive genome of *Daphnia pulex*. *Science* (80-) 331, 555–561.
- Corrêa, S.M., Arbilla, G., 2006. Aromatic hydrocarbons emissions in diesel and biodiesel exhaust. *Atmos. Environ.* 40, 6821–6826.
- Crobeddu, B., Aragao-Santiago, L., Bui, L.C., Boland, S., Baeza Squiban, A., 2017. Oxidative potential of particulate matter 2.5 as predictive indicator of cellular stress. *Environ. Pollut.* 230, 125–133.
- de Souza, C.V., Corrêa, S.M., 2016. Polycyclic aromatic hydrocarbons in diesel emission, diesel fuel and lubricant oil. *Fuel* 185, 925–931.
- Fang, T., Lakey, P.S.J., Weber, R.J., Shiraiwa, M., 2019. Oxidative Potential of Particulate Matter and Generation of Reactive Oxygen Species in Epithelial Lining Fluid. *Environ. Sci. Technol.* 53, 12784–12792.
- Finney, D.J., 1971. *Probit Analysis*, Cambridge University Press. J. Pharm. Sci. 60, 333.
- Fontaras, G., Karavalakis, G., Kousoulidou, M., Ntziachristos, L., Bakeas, E., Stournas, S., Samaras, Z., 2010. Effects of low concentration biodiesel blends application on modern passenger cars. Part 2: impact on carbonyl compound emissions. *Environ. Pollut.* 158, 2496–2503.
- Gali, N.K., Yang, F., Cheung, C.S., Ning, Z., 2017. A comparative analysis of chemical components and cell toxicity properties of solid and semi-volatile PM from diesel and biodiesel blend. *J. Aerosol Sci.* 111, 51–64.
- Godoi, R.H.M., Polezer, G., Borillo, G.C., Brown, A., Valebona, F.B., Silva, T.O.B., et al., 2016. Influence on the oxidative potential of a heavy-duty engine particle emission due to selective catalytic reduction system and biodiesel blend. *Sci. Total Environ.* 560–561, 179–185.
- Guan, C., Cheung, C.S., Li, X., Huang, Z., 2017. Effects of oxygenated fuels on the particle-phase compounds emitted from a diesel engine. *Atmos. Pollut. Res.* 8, 209–220.
- Hedayat, F., Stevanovic, S., Milic, A., Miljevic, B., Nabi, M.N., Zare, A., et al., 2016. Influence of oxygen content of the certain types of biodiesels on particulate oxidative potential. *Sci. Total Environ.* 545–546, 381–388.
- Hemmingsen, J.G., Møller, P., Nøjgaard, J.K., Roursgaard, M., Loft, S., 2011. Oxidative stress, genotoxicity, and vascular cell adhesion molecule expression in cells exposed to particulate matter from combustion of conventional diesel and methyl ester biodiesel blends. *Environ. Sci. Technol.* 45, 8545–8551.
- IARC, WHO, IARC, 2012. Diesel engine exhaust carcinogenic. *World Heal. Organ.* 104, 855–868 Press Release N° 213.
- Jalava, P.I., Salonen, R.O., Nuutinen, K., Pennanen, A.S., Happon, M.S., Tissari, J., et al., 2010. Effect of combustion condition on cytotoxic and inflammatory activity of residential wood combustion particles. *Atmos. Environ.* 44, 1691–1698.
- Jiang, S.Y.N., Yang, F., Chan, K.L., Ning, Z., 2014. Water solubility of metals in coarse PM and PM_{2.5} in typical urban environment in Hong Kong. *Atmos. Pollut. Res.* 5, 236–244.
- Karavalakis, G., Boutsika, V., Stournas, S., Bakeas, E., 2011. Biodiesel emissions profile in modern diesel vehicles. Part 2: effect of biodiesel origin on carbonyl, PAH, nitro-PAH and oxy-PAH emissions. *Sci. Total Environ.* 409, 738–747.
- Karavalakis, G., Fontaras, G., Ampatzoglou, D., Kousoulidou, M., Stournas, S., Samaras, Z., et al., 2010. Effects of low concentration biodiesel blends application on modern passenger cars. Part 3: impact on PAH, nitro-PAH, and oxy-PAH emissions. *Environ. Pollut.* 158, 1584–1594.
- Lapuerta, M., Agudelo, J.R., Prorok, M., Boehman, A.L., 2012a. Bulk modulus of compressibility of diesel/biodiesel/HVO blends. *Energy and Fuels* 26, 1336–1343.
- Lapuerta, M., Armas, O., Rodríguez-Fernández, J., 2008. Effect of biodiesel fuels on diesel engine emissions. *Prog. Energy Combust. Sci.* 34, 198–223.
- Lapuerta, M., Oliva, F., Agudelo, J.R., Boehman, A.L., 2012b. Effect of fuel on the soot nanostructure and consequences on loading and regeneration of diesel particulate filters. *Combust. Flame* 159, 844–853.
- Lee, K.O., Cole, R., Sekar, R., Choi, M.Y., Kang, J.S., Bae, C.S., 2002. Morphological investigation of the microstructure, dimensions, and fractal geometry of diesel particulates. *Proc. Combust. Inst.* 29, 647–653.
- Li, H., Lea-Langton, A., Andrews, G.E., Thompson, M., Musungu, C., 2008. Comparison of exhaust emissions and particulate size distribution for diesel, biodiesel and cooking oil from a heavy duty diesel engine. In: *Proceedings of the SAE World Congress & Exhibition*. Detroit, USA April 14–17.
- Li, X., Zheng, Y., Guan, C., Cheung, C.S., Huang, Z., 2018. Effect of biodiesel on PAH, OPAH, and NPAH emissions from a direct injection diesel engine. *Environ. Sci. Pollut. Res.* 25, 34131–34138.
- Lipsky, E.M., Robinson, A.L., 2006. Effects of dilution on fine particle mass and partitioning of semivolatile organics in diesel exhaust and wood smoke. *Environ. Sci. Technol.* 40, 155–162.
- Liu, H., Barth, M., 2012. Identifying the effect of vehicle operating history on vehicle running emissions. *Atmos. Environ.* 59, 22–29.
- Liu, L., Zhou, Q., Yang, X., Li, G., Zhang, J., Zhou, X., et al., 2020. Cytotoxicity of the soluble and insoluble fractions of atmospheric fine particulate matter. *J. Environ. Sci. (China)* 91, 105–116.
- Liu, Z., Cai, M., Yu, P., Chen, M., Wu, D., Zhang, M., et al., 2018. Age-dependent survival, stress defense, and AMPK in *Daphnia pulex* after short-term exposure to a polystyrene nanoplastic. *Aquat. Toxicol.* 204, 1–8.
- Mahadevan, B., Luch, A., Bravo, C.F., Atkin, J., Stepan, L.B., Pereira, C., et al., 2005. Dibenzo[a,h]pyrene induced DNA adduct formation in lung tissue in vivo. *Cancer Lett.* 227, 25–32.
- Martin, N., Lombard, M., Jensen, K.R., Kelley, P., Pratt, T., Traviss, N., 2017. Effect of biodiesel fuel on “real-world”, nonroad heavy duty diesel engine particulate matter emissions, composition and cytotoxicity. *Sci. Total Environ.* 586, 409–418.
- Martin, N.R., Kelley, P., Klaski, R., Bosco, A., Moore, B., Traviss, N., 2019. Characterization and comparison of oxidative potential of real-world biodiesel and petroleum diesel particulate matter emitted from a nonroad heavy duty diesel engine. *Sci. Total Environ.* 655, 908–914.
- Masih, J., Singhvi, R., Taneja, A., Kumar, K., Masih, H., 2012. Gaseous/particulate bound polycyclic aromatic hydrocarbons

- (PAHs), seasonal variation in North central part of rural India. *Sustain. Cities Soc.* 3, 30–36.
- Mathis, U., Mohr, M., Kaegi, R., Bertola, A., Boulouchos, K., 2005. Influence of diesel engine combustion parameters on primary soot particle diameter. *Environ. Sci. Technol.* 39, 1887–1892.
- Mi, H.H., Lee, W.J., Chen, C.B., Yang, H.H., Wu, S.J., 2000. Effect of fuel aromatic content on PAH emission from a heavy-duty diesel engine. *Chemosphere* 41, 1783–1790.
- Mueller, A., Ulrich, N., Hollmann, J., Zapata Sanchez, C.E., Rolle-Kampczyk, U.E., von Bergen, M., 2019. Characterization of a multianalyte GC-MS/MS procedure for detecting and quantifying polycyclic aromatic hydrocarbons (PAHs) and PAH derivatives from air particulate matter for an improved risk assessment. *Environ. Pollut.* 255, 112967.
- Nikinmaa, M., Suominen, E., Anttila, K., 2019. Water-soluble fraction of crude oil affects variability and has transgenerational effects in *Daphnia magna*. *Aquat. Toxicol.* 211, 137–140.
- Nisbet, I.C.T., LaGoy, P.K., 1992. Toxic equivalency factors (TEFs) for polycyclic aromatic hydrocarbons (PAHs). *Regul. Toxicol. Pharmacol.* 16, 290–300.
- Palacio, I.C., Oliveira, I.F., Franklin, R.L., Barros, S.B.M., Roubicek, D.A., 2016. Evaluating the mutagenicity of the water-soluble fraction of air particulate matter: a comparison of two extraction strategies. *Chemosphere* 158, 124–130.
- Paulo, S., Pereira, G.M., Oraggio, B., Teinilä, K., Custódio, D., Huang, X., Hillamo, R., 2019. A comparative chemical study of PM 10 in three Latin American cities : air Qual. *Atmos. Heal* 12, 1141–1152.
- Pietrogrande, M.C., Bertoli, I., Manarini, F., Russo, M., 2019. Ascorbate assay as a measure of oxidative potential for ambient particles: evidence for the importance of cell-free surrogate lung fluid composition. *Atmos. Environ.* 211, 103–112.
- Pitts, J.N., Van Cauwenberghe, K.A., Grosjean, D., Schmid, J.P., Fitz, D.R., Belser, W.L., 1978. Atmospheric reactions of polycyclic aromatic hydrocarbons: facile formation of mutagenic nitro derivatives. *Science* (80-) 202, 515–519.
- Pourkhesalian, A.M., Stevanovic, S., Salimi, F., Rahman, M.M., Wang, H., Pham, P.X., 2014. Influence of fuel molecular structure on the volatility and oxidative potential of biodiesel particulate matter. *Environ. Sci. Technol.* 48, 12577–12585.
- Ramos-Contreras, C., Concha-Graña, E., López-Mahía, P., Molina-Pérez, F., Muniategui-Lorenzo, S., 2019. Determination of atmospheric particle-bound polycyclic aromatic hydrocarbons using subcritical water extraction coupled with membrane microextraction. *J. Chromatogr. A* 1606, 14–17.
- Ratcliff, M.A., Dane, A.J., Williams, A., Ireland, J., Luecke, J., McCormick, R.L., 2010. Diesel particle filter and fuel effects on heavy-duty diesel engine emissions. *Environ. Sci. Technol.* 44, 8343–8349.
- Ravindra, K., Sokhi, R., Van Grieken, R., 2008. Atmospheric polycyclic aromatic hydrocarbons: source attribution, emission factors and regulation. *Atmos. Environ.* 42, 2895–2921.
- Reitz, R.D., Ogawa, H., Payri, R., Fansler, T., Kokjohn, S., Moriyoshi, Y., et al., 2020. IJER editorial: the future of the internal combustion engine. *Int. J. Engine Res.* 21, 3–10.
- Ringuet, J., Albinet, A., Leoz-Garziandia, E., Budzinski, H., Villenave, E., 2012. Reactivity of polycyclic aromatic compounds (PAHs, NPAHs and OPAHs) adsorbed on natural aerosol particles exposed to atmospheric oxidants. *Atmos. Environ.* 61, 15–22.
- Roig, N., Sierra, J., Rovira, J., Schuhmacher, M., Domingo, J.L., Nadal, M., 2013. In vitro tests to assess toxic effects of airborne PM10 samples. Correlation with metals and chlorinated dioxins and furans. *Sci. Total Environ.* 443, 791–797.
- Rojas, N.Y., Milquez, H.A., Sarmiento, H., 2011. Characterizing priority polycyclic aromatic hydrocarbons (PAH) in particulate matter from diesel and palm oil-based biodiesel B15 combustion. *Atmos. Environ.* 45, 6158–6162.
- Ruiz, F.A., Cadrazco, M., López, A.F., Sanchez-Valdepeñas, J., Agudelo, J.R., Valdepeñas, J., et al., 2015. Impact of dual-fuel combustion with n-butanol or hydrous ethanol on the oxidation reactivity and nanostructure of diesel particulate matter. *Fuel* 161, 18–25.
- Squadrito, G.L., Cueto, R., Dellinger, B., Pryor, W.A., 2001. Quinoid redox cycling as a mechanism for sustained free radical generation by inhaled airborne particulate matter. *Free Radic. Biol. Med.* 31, 1132–1138.
- U.S. Department of Energy, (2004). Alternative Fuels Data Center: biodiesel Blends. Available: <https://afdc.energy.gov/vehicles/diesel.html> Accessed May 4, 2020.
- Velali, E., Papachristou, E., Pantazaki, A., Besis, A., Samara, C., Labrianidis, C., Lialiaris, T., 2018. In vitro cellular toxicity induced by extractable organic fractions of particles exhausted from urban combustion sources - Role of PAHs. *Environ. Pollut.* 243, 1166–1176.
- Vojtisek-lom, M., Czerwinski, J., Leniček, J., Sekyra, M., Topinka, J., Lení, J., et al., 2012. Polycyclic aromatic hydrocarbons (PAHs) in exhaust emissions from diesel engines powered by rapeseed oil methylester and heated non-esterified rapeseed oil. *Atmos. Environ.* 60, 253–261.
- Volta, A., Sforzini, S., Camurati, C., Teoldi, F., Maiorana, S., Croce, A., et al., 2020. Ecotoxicological effects of atmospheric particulate produced by braking systems on aquatic and edaphic organisms. *Environ. Int.* 137, 105564.
- Vu, B., Alves, C.A., Gonçalves, C., Pio, C., Gonçalves, F., Pereira, R., 2012. Mutagenicity assessment of aerosols in emissions from wood combustion in Portugal. *Environ. Pollut.* 166, 172–181.
- Wiersum, U.E., 1996. The formation of polycyclic aromatics, fullerenes and soot in combustion. The mechanism and the environmental connection. *Polycycl. Aromat. Compd.* 11, 291–300.
- Williams, P.T., Bartle, K.D., Andrews, G.E., 1986. The relation between polycyclic aromatic compounds in diesel fuels and exhaust particulates. *Fuel* 65, 1150–1158.
- Zhang, Y., Lou, D., Hu, Z., Tan, P., 2019. Particle number, size distribution, carbons, polycyclic aromatic hydrocarbons and inorganic ions of exhaust particles from a diesel bus fueled with biodiesel blends. *J. Clean. Prod.* 225, 627–636.
- Zou, Y., Jin, C., Su, Y., Li, J., Zhu, B., 2016. Water soluble and insoluble components of urban PM2.5 and their cytotoxic effects on epithelial cells (A549) in vitro. *Environ. Pollut.* 212, 627–635.